Reciprocal inflammatory signals establish profibrotic cross-feeding metabolism

Authors

Preeti Yadav[1,2]*, Javier Gómez Ortega[1,2]*, Kai-chun Chang[3], Sixuan Pan[3], Nivedita Biswas[1,2], Julia Nilsson[4], Xiaoyang Yin[1,2,5], Aritra Bhattacharyya[1,2], Kaveh Boostanpour[1,2], Tatsuya Tsukui[1,6], Dean Sheppard[1,6], Baosheng Li[5], Mazharul Maishan[1], Hiroki Taenaka[1], Michael A. Matthay[1], Rieko Muramatsu[7], Mohammad Naser[8], Ari B. Molofsky[4], Paul J. Wolters[1], Adam R. Abate[3], Kevin M. Tharp[9], Mallar Bhattacharya[1,2§]

* Equal contribution

Affiliations

[1] Division of Pulmonary, Critical Care, Allergy, and Sleep, Department of Medicine, University of California, San Francisco, San Francisco, CA, USA

[2] Sandler Asthma Basic Research Center, University of California, San Francisco, San Francisco, CA, USA

[3] Department of Bioengineering and Therapeutic Sciences, University of California, San Francisco, San Francisco, CA, USA

[4] Department of Laboratory Medicine, University of California, San Francisco, San Francisco, CA, USA

[5] Department of Radiation Oncology, Shandong Cancer Hospital and Institute, Shandong First Medical University and Shandong Academy of Medical Sciences, Jinan, China

[6] Cardiovascular Research Institute; University of California, San Francisco, San Francisco, CA, USA

[7] Department of Molecular Pharmacology, National Institute of Neuroscience, National Center of Neurology and Psychiatry, Kodaira, Japan

[8] UCSF CoLabs, University of California, San Francisco, San Francisco, CA 94143, USA

[9] Center for Bioengineering and Tissue Regeneration, Department of Surgery, University of California, San Francisco, San Francisco, CA, USA

Contact Info

§ Correspondence: mallar.bhattacharya@ucsf.edu

Summary

When monocyte-derived macrophages are recruited to injured tissues, they can induce a maladaptive fibrotic response characterized by excessive production of fibrillar collagen from local fibroblasts. Macrophages initiate the fibrotic programming of fibroblasts via paracrine factors, but it is unclear if reciprocal responses from the fibroblasts trigger pro-fibrotic programming of macrophages to establish a collaborative feed-forward fibrotic circuit. We identify macrophage-fibroblast cross talk necessary for injury-associated fibrosis, in which macrophages induce interleukin 6 (*IL-6*) expression in fibroblasts via purinergic receptor P2rx4 signaling and IL-6 induces arginase 1 (*Arg1*) expression in macrophages. Surprisingly, *Arg1* contributes to fibrotic responses by metabolizing arginine to ornithine, which fibroblasts use as a substrate to synthesize proline, a uniquely abundant constituent of fibrillar collagen. Taken together, we define a bidirectional circuit between macrophages and fibroblasts that facilitates cross-feeding metabolism necessary for injury-associated fibrosis.

Main

Pathologic fibrosis is a destructive response to tissue injury that results from deposition of excess fibrillar collagen by activated fibroblasts. Recent studies have revealed a heterogeneity of fibroblast states following injury, and inflammatory fibroblasts have been detected as a distinct subset of mesenchymal cells present in the early period after injury prior to the onset of full-blown fibrosis[1-3]. How cytokine expression by inflammatory fibroblasts regulates fibrogenesis is not well understood.

51 The early phase of injury is also marked by influx of monocyte-derived macrophages, which
52 localize to fibroblasts at sites of injury[4]. Several studies have shown that these monocyte-derived
53 macrophages signal to fibroblasts via paracrine mediators[4-6], but the fibroblast responses are not well
54 characterized. Here, we identify a paracrine circuit between macrophages and fibroblasts that is
55 established in the late inflammatory phase following tissue injury. In a tissue injury model, macrophage-
56 derived extracellular ATP drove fibroblast IL-6 expression. IL-6, in turn, induced macrophage
57 expression of Arg1, which was necessary for lung collagen production via ornithine metabolism by
58 activated fibroblasts.
59
60 ***Macrophages induce fibroblast IL-6***
61 To screen for macrophage-dependent secreted factors expressed by fibroblasts, we analyzed
62 scRNAseq data from cocultures of primary lung macrophages and fibroblasts, or fibroblasts cultured
63 alone (**Figure 1a-b, Figure S1a-b**). This analysis revealed the induction of multiple clusters unique to
64 fibroblasts cocultured with macrophages (**Figure 1c**). Notably, these clusters had higher levels of a
65 gene signature for collagen genes (**Figure S1c, Table S1**), consistent with the pro-fibrotic effects of
66 macrophage coculture. Focusing analysis on secreted factors[7], we also noted high expression of the
67 cytokine IL-6 in macrophage coculture-specific fibroblast clusters (**Figure 1d**; **Figure S2a**). IL-6 has
68 emerged as a target for the treatment of lung fibrosis[8-11]. Analysis of scRNAseq time course data for
69 multiple lung cell types in the bleomycin model confirmed that IL-6 was most highly expressed in
70 fibroblasts *in vivo* (**Figure 1e**), with some expression also noted in other mesenchymal cells such as
71 smooth muscle cells and pericytes (**Fig S2b**). We then confirmed macrophage-dependent fibroblast IL-
72 6 induction in human lung cell cocultures (**Fig S2c**).
73 To determine the mechanism of IL-6 induction in fibroblasts, we interrogated GO datasets under
74 the category of “Cellular Response to Stimulus”. This analysis revealed that the GO pathway “Cellular
75 Response to ATP” was enriched in fibroblasts when they were cocultured with macrophages (**Figure
76 1f**). This GO pathway is relevant because extracellular ATP (eATP) levels are elevated in the

77 bronchoalveolar lavage fluid of patients with idiopathic pulmonary fibrosis (IPF)[12], and fibroblast-specific
78 deletion of the eATP receptor P2rx4 in mice suppresses injury-induced fibrosis[13]. To test if eATP
79 signaling via P2rx4 regulates IL-6 expression, we assayed IL-6 levels by ELISA of conditioned media
80 from cocultures of WT macrophages with either WT or P2rx4 knockout (KO) fibroblasts, finding that IL-6
81 was decreased in the case of P2rx4 KO fibroblasts (**Figure 1g**). Direct treatment of cultured murine
82 lung fibroblasts with ATPγS, a nonhydrolyzable form of ATP, increased IL-6 in the conditioned media of
83 WT but not P2rx4 KO lung fibroblasts (**Fig S2d**). This effect was blocked by inhibition of p38 Map
84 Kinase, which has been shown to mediate P2rx4 signaling[14,15] (**Fig S2e**). Importantly, mice with
85 fibroblast-specific P2rx4 KO had decreased bronchoalveolar lavage IL-6 compared to wild type
86 following bleomycin injury (**Figure 1h**). Consistent with the importance of IL6 to the fibrotic response
87 after injury, we confirmed that IL6 KO mice were protected from lung fibrosis (**Fig S2f-g**). To test
88 whether macrophages were the source of the eATP found to induce IL-6, we treated mice with
89 liposomal clodronate by airway delivery after injury for ablation of macrophages. The number of
90 CD11b+CD64+ macrophages was significantly decreased with macrophage ablation, which also
91 significantly decreased lung lavage ATP levels (**Figure 1i-k**). Taken together, these data indicate that
92 eATP derived from macrophages induces fibroblast IL-6 via P2rx4.
93
94 ***Fibroblast P2rx4-dependent IL-6 regulates macrophage Arg1***
95 We next examined whether eATP-mediated IL-6 production in fibroblasts might reciprocally regulate
96 macrophage profibrotic responses. We performed differential gene expression analysis from scRNAseq
97 data for WT macrophages cultured with either WT or P2rx4 KO fibroblasts. The top differentially
98 expressed gene was *Arg1*, and its expression was dependent on fibroblast P2rx4 expression (**Figure**
99 **2a**). We hypothesized that fibroblast-derived IL-6, which was decreased in P2rx4 KO fibroblasts, may
100 regulate macrophage *Arg1* expression as found in other systems[16]. Analysis of ligand-receptor
101 interaction via CellChat[17] and Ingenuity Pathways Analysis confirmed suppression of IL-6 signaling in

102 the P2rx4 KO condition (**Figure S3a**). We then confirmed an increase of Arg1 in both cellular lysates
103 and conditioned media of cultured lung macrophages treated with IL-6 (**Figure 2b**).
104 Interestingly, analysis of a published scRNAseq time course following bleomycin lung injury[18]
105 showed maximal *Arg1* in cells annotated to be similar to the C2 transitional macrophage compartment
106 we previously demonstrated to localize to the fibrotic niche after injury[4] (**Figure 2c; Figure S3b**). C2
107 cells not only expressed higher Arg1 but also expressed higher levels of the Fab5 markers that were
108 recently found to be associated with pro-fibrotic macrophages in both mouse and human fibrotic lung
109 and liver datasets[19] (**Figure S3b**). Similar to our previous findings for these transitional cells[4], Arg1+
110 cells were found in proximity to clusters of activated fibroblasts that form after injury (**Figure 2d**), and
111 flow cytometry confirmed *Arg1* expression in CD11b+CD64+ macrophages as opposed to monocytes,
112 alveolar macrophages, or dendritic cells (**Figure S4**). Taken together, these data indicate that fibroblast
113 IL-6 regulates macrophage *Arg1* expression in the fibrotic period post injury, and *Arg1*+ cells localize to
114 sites of fibroblast accumulation and activation.
115
116 ***Arg1 regulates lung fibrosis***
117 Arg1 is a marker of alternatively activated macrophages, but studies of its functional role in fibrosis are
118 limited. Thus, we first treated bleomycin-injured mice with the Arg1 inhibitor CB-1158[20] during the early
119 fibrotic period and found that lung collagen content was significantly decreased and weight recovery
120 improved (**Figure 3a, Figure S5a**). In macrophage-specific Arg1 heterozygous KO mice, lung collagen
121 content and arginase activity were likewise decreased after injury (**Figure 3b**). To further test the
122 clinical significance of *Arg1*+ macrophages, we performed scRNAseq analysis of aged mice compared
123 to young given that aging is a major risk factor for the development of lung fibrosis in patients.
124 Remarkably, *Arg1*+ macrophages were not only greatly increased in bleomycin-injured aged mice but
125 also co-expressed the Fab5 profibrotic macrophage genes[19] (**Figure 3c; Fig S5b**). We then labeled
126 clinical lung samples from IPF by immunofluorescence. ARG1+ cells co-expressing the macrophage
127 marker CD163+ were notably increased in fibrotic regions defined by Masson's trichrome stain for

128 collagen (**Figure 3d**). Single-cell transcriptomic analysis also confirmed that ARG1 was expressed in
129 CD163+ monocytes and macrophages in human lungs (**Fig S5c**), and analysis of a dataset of BAL cell
130 gene expression by microarray[21] confirmed higher expression in IPF (**Fig S5d**). To test ARG1 as a
131 potential profibrotic factor in human fibrosis, we prepared precision cut lung slices and treated them
132 with CB-1158 or the IL6RA-blocking antibody tocilizumab for 24 hours. Collagen expression was
133 decreased with both treatments compared to untreated slices, suggesting inhibition of new collagen
134 synthesis (**Figure 3e**).
135
136 ***Arg1 regulates availability of ornithine, a pro-fibrotic substrate***
137 Arg1 enzymatically converts arginine to urea and ornithine, and macrophages expressing *Arg1* secrete
138 ornithine into the tissue microenvrionment[22]. Ornithine can serve as a substrate for the synthesis of
139 proline[23], a major constituent of collagens. Thus, we sought to determine if *Arg1*+ macrophages supply
140 ornithine as a substrate for collagen production by fibroblasts. First, consistent with a potential for
141 ornithine to drive collagen production, we found that exogenous ornithine increased fibroblast collagen
142 expression at the protein level (**Figure S5e**). Next, in alignment with our transcriptomic findings, Col1a1
143 was increased in cocultures relative to fibroblast monocultures by immunofluorescence analysis
144 (**Figure 4a**). Importantly, fibroblasts with deletion of IL-6 or P2rx4, as well as Arg1 inhibition with CB-
145 1158, decreased collagen expression compared to WT, untreated cocultures (**Figure 4a**). Mass
146 spectrometric analysis confirmed that Arg1 inhibition with CB-1158 both increased arginine and
147 decreased ornithine in macrophages, and in fibroblasts the level of proline was correspondingly
148 decreased (**Figure 4b**). To verify that ornithine can be used as a substrate for proline synthesis, we
149 treated fibroblasts in culture with $^{13}C_5$-ornithine and detected an m + 5 mass shift in proline ($^{13}C_5$
150 proline), consistent with conversion of ornithine to proline via the pyrroline 5-carboxylate (P5C)
151 intermediate (**Figure 4c**). We then treated mice injured with bleomycin with or without ornithine by oral
152 gavage twice daily during the fibrotic phase after injury and found that ornithine treatment significantly
153 increased lung collagen content (**Figure 4d**).

154 Single cell profiling has enabled the identification of markers for scar-associated macrophages
155 (SAM)[24] as well as for disease-associated fibroblasts[3], but the functional interactions of these cells are
156 not well understood. We have demonstrated a role for eATP, a damage-associated molecular pattern
157 associated with inflammation and derived from macrophages, in the initiation of pathologic bidirectional
158 signaling—specifically in the induction of fibroblast IL-6 after injury. IL-6 is a key determinant of multiple
159 lung phenotypes including alveolar epithelial mobilization and self-renewal[25,26] and can induce
160 macrophage alternative activation during tissular inflammation[27]. Our results reveal the importance of
161 IL-6 for induction of Arg1 in transitional macrophages present in the fibrotic niche. Moreover, we find
162 that Arg1 regulates macrophage production of ornithine, which increases collagen protein expression in
163 fibroblasts *in vitro* and *in vivo*. These results reveal a previously unrecognized metabolic requirement of
164 macrophage ornithine for fibrogenesis via conversion to proline, an essential collagen building block,
165 though we note that ornithine conversion to polyamines with profibrotic potential remains a further
166 possibility not yet addressed by our work. Future studies should focus on how this circuit is abated in
167 the resolution of fibrosis, and whether it remains entrenched in progressive cases leading to organ
168 failure.
169

170 **Methods**

171 ***Human lung tissues***

172 The studies described in this paper were conducted according to the principles of the Declaration of
173 Helsinki. IPF lung samples were obtained as explants at the time of lung transplantation. Written,
174 informed consent was obtained from all subjects, and the study was approved by the University of San
175 Francisco, California institutional review board. Deceased donor control lungs not known to have lung
176 disease were made available by Donor Network West. Because these samples were acquired from
177 deceased individuals the study is not considered human subjects research as per UCSF and NIH
178 policy.
179

180 ***Mice***

181 Pdgfrb-Cre[28], Lysm-Cre[29], P2rx4 floxed[30], Arg1 floxed[31], and Arg1-YFP[32] mice were available to the
182 investigative team, and IL-6 KO[33] and WT mice were obtained from JAX. Col1a1-GFP mice were
183 obtained from David Brenner[34]. All mice were maintained on a C57BL/6 background and were
184 maintained in specific pathogen-free animal barrier facility at the University of California, San Francisco.
185 All experiments were performed on 6-8 weeks old, sex-matched mice, or in the case of aged mice, 24-
186 month-old, sex-matched mice, and were performed in accordance with approved protocols by the
187 University of California, San Francisco Institutional Animal Care and Use Committee.

188

189 ***Mouse lung injury, cell isolation, and macrophage-fibroblast coculture***

190 For lung injury, mice anesthetized with isoflurane were instilled intratracheally with bleomycin
191 (Fresenius, 3U/Kg), and lungs were isolated after 7 days after injury. In the case of Arg1 inhibition,
192 bleomycin-injured mice were treated daily from day 9 to day 15 post-injury with 100 mg/kg CB-1158
193 (Numidargistat dihydrochloride) dissolved in water, by oral gavage. In the case of ornithine treatment,
194 mice were treated daily by gavage with ornithine 2 mg/kg dissolved in 100 μL of water. For creation of
195 single cell suspensions, lungs were harvested from euthanized mice and minced with scissors, the
196 tissue was resuspended in RPMI with 0.2% Collagenase (10103586001, Roche), 2000 U/ml DNase I
197 (4716728001, Roche) and 0.1 mg/ml Dispase II (4942078001, Sigma). The suspension was incubated
198 for 1 hour at 37°C and passed through a 70 μm filter (130-110-916, MACS SmartStrainers) to obtain
199 single cells. The cells were washed twice with 1X PBS pH 7.4 (10010023, Gibco). For macrophage
200 isolation, a total of 10^7 cells were resuspended in 80μl PBS buffer supplemented with 0.5% BSA (0332,
201 VWR Life Science) and 2mM EDTA (E57040, Research Products International). 20μl CD11b
202 microbeads were used per 10^7 cells. Macrophages were obtained by positive selection by binding to
203 CD11b microbeads and passing through MACS columns (130-049-601, Miltenyi Biotech). Isolated
204 $CD11b^+$ macrophages were cultured in DMEM supplemented with 10% FBS, 1% penicillin-

205 streptomycin, and 20 ng/ml M-CSF (315-02, Peprotech) for 2 days. Primary mouse lung fibroblasts
206 were freshly isolated after magnetic bead-based negative selection of epithelial cells (118204, Biotin
207 anti-mouse CD326 Epcam, Clone: G8.8, BioLegend), endothelial cells (102404, Biotin anti-mouse
208 CD31, clone: 390), immune cells (103104, Biotin anti-mouse CD45, clone: 30-F11, BioLegend),
209 pericytes and smooth muscle cells (134716, Biotin anti-mouse CD146, clone: ME-9F1, BioLegend), and
210 red blood cells (116204, Biotin anti-mouse Ter119, clone: TER-119, BioLegend) with biotinylated
211 antibodies and Dynabeads (MyOne Streptavidin T1, 65601, Thermo Fisher Scientific) as previously
212 described[1]. Fibroblasts were cultured for 5 days prior to trypsinization and addition to macrophages for
213 coculture at a 1:1 ratio in DMEM complete media for 5 further days.
214
215 ***Human lung cell isolation and macrophage-fibroblast coculture***
216 Human lung tissue from deceased donors not used for transplant was resected and minced in Hanks'
217 Balanced Salt Solution (HBSS) buffer supplemented with 0.2% Collagenase (10103586001, Roche),
218 2000 U/ml DNase I (4716728001, Roche) and 0.1 mg/ml Dispase II (4942078001, Sigma), 1%
219 Penicillin-streptomycin for 1.5 hours at 37°C and 5% CO2. 1X Amphotericin B (15290026, Gibco) was
220 added to the dissociation solution for 30 min. Digested lung tissue was lysed further with a MACS
221 tissue dissociator (gentleMACS Dissociator, Miltenyi Biotec) using gentleMACS C tubes (130-093-237,
222 Miltenyi Biotec) at mLUNG-01 setting. The suspension was then passed through a 70 μm filter to obtain
223 single cells. Cells were resuspended in PBS with 0.5% BSA and 2mM EDTA. Macrophages were
224 incubated with CD11b microbeads and loaded on MACS columns. After washing the cell fraction of
225 unlabeled cells, CD11b+ cells were eluted and cultured in DMEM supplemented 10% FBS (10082147
226 Gibco), 1% penicillin-streptomycin (1670249, MP Biomedicals), and 50 ng/ml human M-CSF (300-25,
227 Peprotech) for 2 days. For the negative selection of human fibroblasts, the following antibodies were
228 used at a 1:200 ratio: epithelial cells (324216, Biotin anti-human Epcam, clone:9C4, BioLegend),
229 endothelial cells (13-0319-82, Biotin anti-human CD31, clone: WM-59, Invitrogen), immune cells

230 (368534, Biotin anti-human CD45, clone: 2D1, BioLegend), pericytes and smooth muscle (361036,
231 Biotin anti-human CD146, clone: P1H12, BioLegend). Fibroblasts were cultured in DMEM
232 supplemented with 10% serum, 1% penicillin-streptomycin, and 1% amphotericin B.
233
234 ***Flow cytometry***
235 *Cocultured cells:* Cocultures were trypsinized with 0.25% trypsin and resuspended in 1X PBS with 0.5%
236 BSA and 2mM EDTA. Single-cell suspensions were pre-stained with Fc blocker for 10 min in ice
237 followed by staining at 1:300 with anti-CD64 (139304, PE anti-mouse CD64, clone:X54-5/7.1,
238 BioLegend) and anti-Pdgfra (25-1401-82, PE-Cy7, anti-mouse CD140a, clone: APA5, Invitrogen)
239 antibodies for 40 min. DAPI was used to distinguish dead cells.
240 *Mouse lung cell suspensions (for clodronate macrophage depletion experiments):* Single cell
241 suspensions from digested mice lungs were incubated with ghost dye 516 (13-0867-T100, TONBO)
242 1:300 for 30min in ice followed by washing with staining buffer consisting of 1% EDTA and 1% serum in
243 PBS. Cells were stained with anti-CD64 (139304, PE anti-mouse CD64, clone:X54-5/7.1, BioLegend)
244 and anti-CD11b (25-0112-81, PE-Cy7, clone:M1/70, eBioscience) antibodies for 40 min at 4°C
245 protected from light. Cells were washed with staining buffer and resuspended in 100μl staining buffer
246 and 100μl IC fixation buffer. Samples were kept in dark at 4°C overnight followed by resuspending in
247 300μl staining buffer. Data was acquired using Fortessa (BD Bioscience) and analyzed using FlowJo
248 software.
249 *Mouse lung cell suspension (for experiments with Arg1-YFP mice):* Whole lung single cell suspensions
250 were prepared by harvesting lung lobes into 5 ml HBSS with 40μl Liberase Tm (0.1 U/ml, Roche, Cat#
251 5401127001) and 20μl DNAse 1 (10mg/ml, Roche, Cat# 10104159001), followed by automated tissue
252 dissociation (GentleMacs; Miltenyi Biotec) and tissue digestion for 30 min at 37°C on a shaker.
253 Digested samples were processed on the GentleMacs using the “lung2” program, passed through
254 70μm filters, and washed, followed by red blood cell lysis and final suspension in FACS buffer. Cells

255 were counted using a NucleoCounter (Chemometic). All samples were stained in 96-well V-bottom
256 plates. Single cell samples were first incubated with antibodies to surface antigens for 30 min at 4°C in
257 50µl staining volume. Flow cytometry was performed on BD LSRFortessa X-20. Fluorochrome
258 compensation was performed with single-stained UltraComp eBeads (Invitrogen, Cat# 01-2222-42).
259 Samples were FSC-A/SSC-A gated to exclude debris, followed by FSC-H/FSC-A gating to select single
260 cells and Draq7 viability dye (Biolegend) to exclude dead cells. Early transitional macrophages (TMs)
261 were identified as $CD19^-$, $Ly6G^-$, $NK1.1^-$, Siglec-F^-, $CD11b^+$,$CCR2^+$ and $CD64^+$. Late TMs were
262 identified as $CD19^-$, $Ly6G^-$, $NK1.1^-$, Siglec-F^-, $CD11b^+$, $CCR2^-$ and $CD64^+$. GR1 MDSC were identified
263 as $CD19^-$, $Ly6G^+$, $CD64^-$ and $CD11c^+$. Arginase1 positive cells were identified by the presence of eYFP.
264 Data were analyzed using FlowJo software (TreeStar, USA) and compiled using Prism (GraphPad
265 Software). Monoclonal antibodies used were: anti-CD45 (30-F11, Biolegend), anti-CD11b (M1/70,
266 Biolegend), anti-CD11c (N418, Biolegend), anti-NK1.1 (PK136, Biolegend), anti-CD19 (6D5,
267 Biolegend), anti-T1/ST2 (DJ8, BD BioSciences), anti-MerTK (DS5MMER, eBiosciences), anti-CD64
268 (X54-5/7, eBiosciences), anti-Ly6C (HK1.4), anti-Ly6G (1A8, Biolegend), anti-SiglecF (E50-2440), and
269 anti-I-A/I-E (MHCII) (M5/114.15.2, Biolegend), anti-CCR2 (475301, BD BioSciences).
270

271 ***Quantitative Real-Time PCR analysis***

272 Macrophages or fibroblasts were lysed in 300µl TRIzol reagent (10296010, Ambion life technologies) to
273 obtained RNA. 600 ng of RNA per sample was used to prepare cDNA using iScript reverse
274 transcriptase supermix (Bio-Rad, 1708841). qPCR was performed for the target genes using SYBR
275 Green super mix (Applied Biosystems, 4309155). Gene expression was normalized to Gapdh for
276 analysis of mouse transcripts or 18S rRNA for human.

277 Mouse *Gapdh* Forward: AGTATGACTCCACTCACGGCAA

278 Mouse *Gapdh* Reverse: TCTCGCTCCTGGAAGATGGT

279 Mouse *IL6* Forward: CCAAGAGGTGAGTGCTTCCC

280 Mouse *IL6* Reverse: CTGTTGTTCAGACTCTCTCCCT

281 Human 18S rRNA Forward: GTAACCCGTTGAACCCCATT

282 Human 18S rRNA Reverse: CCATCCAATCGGTAGTAGCG

283 Human IL6 Forward: ACTCACCTCTTCAGAACGAATTG

284 Human IL6 Reverse: CCATCTTTGGAAGGTTCAGGTTG

285

286 ***ATP measurement***

287 For ATP measurement, 1 mL of mouse lung lavage was collected in 1X PBS containing 100μM
288 ATPase inhibitor. ATP measurement was performed immediately by measuring bioluminescence using
289 Biotek H1 plate reader as described in the manufacturer's protocol (A22066, ATP determination Kit,
290 ThermoFisher Scientific). Briefly, an assay solution was prepared by mixing a working concentration of
291 10μM dithiothreitol, 0.2mM D- luciferase, 7.5 μg/ml firefly luciferase in 1X reaction buffer diluted with
292 distilled water. The reaction was kept in ice and protected from light. 10 μl of sample was mixed with 90
293 μl of assay solution, and light emission was measured at 560 nm using a Biotek plate reader.

294

295 ***Macrophage depletion***

296 Mice were treated 6 days after bleomycin lung injury with 100μl of 18.4 mM liposomal-clodronate (CLD-
297 8909, Encapsula NanoSciences) by oral aspiration. Mice were kept under observation for 24hrs. These
298 mice were euthanized on day 7, and bronchoalveolar lavage fluid was collected in PBS containing
299 100μM ATPase inhibitor, and lung cell suspensions were prepared for flow cytometry.

300

301 ***IL-6 ELISA***

302 Bronchoalveolar lavage fluid or conditioned culture media were collected for measurement of IL-6 with
303 a Duoset ELISA kit (R&D Systems, DY406-05). Capture antibody was coated overnight in a 96 well
304 plate at room temperature. Wells were aspirated and washed in ELISA wash buffer and blocked by
305 adding reagent diluent consisting of 1% BSA in PBS. After 1 hour of room temperature incubation, wells

306 were again washed with wash buffer and samples or standards were added and incubated for 2 hours
307 at room temperature. Detection antibody was used along with streptavidin-HRP and substrate solution.
308 The reaction was stopped with stop solution, and optical density was measured using a microplate
309 reader at 450 nm.
310
311 ***Arginase 1 ELISA***
312 CD11b+ mouse lung cells were seeded in 12-well dishes for 2 days in DMEM supplemented with M-Csf
313 (315-02, Peprotech). Cells were stimulated with murine IL-6 for 72 hours. Conditioned media Arginase
314 1 levels were measured using Mouse Arginase 1 ELISA Kit (ab269541, Abcam) based on the
315 manufacturer's protocol. Briefly, 50 µl of the undiluted samples were added to each well along with 50µl
316 of antibody cocktail, which consisted of capture antibody and detection antibody dissolved in antibody
317 diluent. Plates were incubated for 1 hour at room temperature. Wells were washed thrice with wash
318 buffer and incubated with 100 µl Tetramethylbenzidine (TMB) substrate for 15 min. The reaction was
319 stopped using 100µl stop solution, and OD was measured at 450nm.
320
321 ***Histology and Immunofluorescence imaging***
322 *Mouse lung:* Mouse lungs were fixed in 4% formaldehyde at 4°C for 4 hours, then washed and
323 submerged in 30% sucrose solution overnight at 4°C. Next, the tissue was incubated in 1:1 solution of
324 30% sucrose and OCT (4585, OCT) overnight followed by changing to OCT for 2 hours, and then a
325 tissue block was frozen after embedding in OCT. 15 µm sections were cut from OCT-embedded tissue.
326 For immunofluorescence imaging, sections were first pretreated with 1X target antigen retrieval
327 reagents (RNAscope, advanced cell diagnostics) at 100° C for 10 min. Dried slides were incubated with
328 anti-Arg1 primary antibody (93668, Cell Signaling Technology) overnight at 4° C in antibody staining
329 solution containing 1% BSA, 1% Tween20 and 2% serum. Slides were washed thrice with PBS and
330 incubated with secondary antibodies goat anti-mouse IgG 647 and donkey anti-rabbit IgG 555 for 4

331 hours at 4°C. The sections were washed in PBS and mounted on antifade DAPI mounting media and
332 imaged using Leica SP8 confocal laser scanning microscope at BIDC, UCSF.
333 For Sirius Red imaging, sections prepared from mouse lungs frozen in OCT were stained with
334 Sirius Red (0.1% Sirius Red in saturated picric acid, Electron Microscopy Sciences, 26357-02) for 60
335 min followed by a 2-min 0.01 N HCl wash, rinsed in 70% ethanol, and air-dried overnight before
336 imaging. Images were acquired using a bright-field microscope (Zeiss Axio scan.Z1). The images were
337 quantified using Qupath image analysis software using the artificial neural network pixel classifier
338 function[35], with software training based on user-defined fibrotic regions in a single image.
339 *Human lung:* 4 μm thick sections from patient FFPE blocks were collected for IHC staining. Slides were
340 stained on the Discovery Ultra automated platform (Roche Diagnostics) using Ventana reagents unless
341 otherwise stated. After deparaffinization, antigen retrieval was performed in CC1 at 97C for 32min.
342 Primary antibodies were applied sequentially as CD163 (EPR19518, Abcam, ab182422, 1:250) and
343 Arginase-1 (SP156, Roche, 760-4801, pre-diluted) and paired with R6G and Cy5 respectively. The
344 slides were then scanned using with a 20x objective on AxioScan (Zeiss) whole slide scanner.
345 Masson's Trichrome staining was performed using the 2000™ kit (StatLab, SKU #: KTMTR2 EA)
346 following manufacturer's instructions. QuPath image analysis software[35] was used to define fibrotic
347 regions by thresholding using Masson's trichrome stain-defined regions.
348 *Coculture:* Mouse macrophages and fibroblasts were cocultured, or in some cases fibroblasts cultured
349 alone, on glass coverslips (10 mm, Carolina). Treatments included 1mM ornithine (020040-100,
350 Research Products International) for 2 days after 3 days of culture, or 100nM CB1158 (HY-101979A,
351 MedChemExpress) for 24 hours after 4 days of coculture. Cells were fixed with 4% formaldehyde for 10
352 min at room temperature followed by washing thrice with 1X PBS. Col1a1 antibody (72026, Cell
353 Signaling Technology) was diluted in 1% BSA and 0.5% Triton X100 antibody staining solution. Imaris
354 software (Oxford Instruments) was used to quantify fluorescence.
355

356 ***Arginase activity assay***

357 Whole lung lysates were prepared for arginase activity assay per the vendor protocol (Abcam,
358 ab180877). Briefly, lysates were incubated for 20 minutes at 37°C with substrate solution followed by
359 addition of reaction mix and developer. Absorbance was measured on a microplate reader (Bio Tek
360 Synergy H1) at OD = 570 nm at 37°C.

361

362 ***Western blot***

363 Precision cut lung slices were obtained from human IPF tissue sections. Briefly, IPF tissue was injected
364 with 2% low melting agarose (50111, Lonza) and then submerged in ice-cold PBS to allow solidification
365 of agarose. 400 µm lung slices was generated using Compresstome (VF-310-OZ, Precisionary
366 Instruments). Slices were kept in complete DMEM media for 2 hours to allow the release of agarose
367 followed by changing to fresh complete DMEM. Lung slices were treated with 50 μM CB1158 or 10
368 μg/ml Tocilizumab for 24 hours. After incubation slices were minced using a tissue homogenizer. Cells
369 were lysed in Pierce RIPA buffer (Thermo Fisher Scientific, 89901) with protease inhibitor cocktail
370 (Thermo Fisher Scientific, 1861278). 10 µg of protein was run on 10% sodium dodecyl sulfate-
371 polyacrylamide gel electrophoresis (Bio-rad, 4561034) and transferred to a PVDF membrane (Thermo
372 Fisher Scientific, 88520). The membrane was incubated with 1:1000 Col1a1(#720265, Cell Signaling
373 Technology) overnight at 4°C. Blots were washed in 1XTBST and incubated with peroxidase-
374 conjugated goat anti-rabbit (1:20,000, Anaspec, AS28177) for 4 hr at 4°C. These blots were developed
375 using SuperSignal West Pico Chemiluminescent substrate (Thermo Fisher Scientific, 34080) in
376 ChemiDoc XRS+ gel imaging system (Bio-rad). Quantification of bands was done using ImageJ.

377

378 ***Hydroxyproline assay***

379 Mice were euthanized and lungs were excised and snap frozen. Isolated lung samples were
380 homogenized and incubated with 50% trichloroacetic acid (T6399, Sigma) on ice for 20 min. Samples

381 were then incubated in 12N HCL (A144, Fisher) overnight at 110°C. Dried pellets were reconstituted in
382 distilled water with constant shaking for 2 hours at room temperature. Samples were then mixed with
383 1.4% Chloramine T (Sigma, 85739) and 0.5 M sodium acetate (Sigma, 241245) in 10% 2-propanol
384 (Fisher, A416) and incubated with Ehrlich's solution (Sigma, 03891) for 15 min at 65°C. Absorbance
385 was quantified at 550 nm, and concentration was calculated using a standard curve of commercial
386 hydroxyproline (Sigma, H5534).
387
388 ***scRNAseq library preparation and sequencing***
389 PIPseq T2 3' Single Cell RNA Kit (v3.0 – cultured cells, v4.0 – directly sequenced cells) was used for
390 pre-templated instant partitioning (PIP) to capture single-cell mRNA transcripts with PIP beads
391 according to manufacturer's protocol (Fluent Biosciences, FB0001026). In the case of directly
392 sequenced cells, 7 days after bleomycin injury, cells were isolated by the isolation procedure described
393 above for scRNAseq workflow. In the case of cocultures, 7 days after bleomycin lung injury, mice were
394 euthanized and lungs were harvested followed by cell isolation as above. After 5 days of coculture,
395 single cell suspension of cells was obtained by trypsinization followed by washing in 1X PBS.
396 Cells were washed in ice-cold PIPseq Cell Suspension Buffer (Fluent Biosciences, FB0002440).
397 Cells were counted and stained with Trypan blue to confirm >90% viability. Single-cell library
398 preparation was performed using the manufacturer-recommended default protocol and settings. The
399 sequencing libraries were submitted to UCSF Center for Advanced Technology (Novaseq X) or
400 Novogene (Novaseq 6000) for sequencing. The demultiplexed FASTQ files were aligned to mouse
401 genome (mm10) using PIPseeker 1.0.0 (Fluent Biosciences). After sequence alignment, we observed
402 around 50% of input cells being called when PIPseeker sensitivity level was set to 3, which was near
403 the inflection point of the barcode rank plot. The original FASTQ files, the quality reports, and the
404 expression matrix outputs of PIPseeker have been deposited in Gene Expression Omnibus (GEO).
405
406 ***scRNAseq Data Analysis***

407 The Seurat – Guided Clustering Tutorial (March 27, 2023) was followed to convert our expression
408 matrixes into Seurat objects (Seurat version 4.3.0)[36]. For quality control, we removed the cells with less
409 than 200 genes or more than 10,000 genes and larger than 5% mitochondrial content. Seurat objects
410 were integrated following Seurat's Introduction to scRNAseq Integration (March 27, 2023), selecting the
411 top 2,000 variable features as integration anchors. Cell doublets were removed with the package
412 DoubletFinder (2.0.3)[37]. Following Seurat – Guided Clustering Tutorial (March 27, 2023), we selected
413 the top 2000 highly variable genes to obtain the cell UMAP coordinates and group the cells into clusters
414 with a sensitivity of 0.5[36]. Cell types were annotated using the SingleR package 1.10.04[4] using the
415 ImmGen database[38] as reference. The Gene Set Enrichment Analysis (GSEA) was performed using
416 the package enrichR 3.1[39] (FDR<0.05), with gene ontology data taken from the database
417 "GO_Biological_Process_2021"[40]. Cell communication pathways analysis was performed using the
418 package CellChat (1.6.1)[17]. Upstream regulator prediction was done using the Ingenuity Pathway
419 Analysis software (Qiagen)[41]. Differentially expressed genes for macrophages with $p < 0.05$ and
420 average log2 fold change > 0.75 were used for analysis. Analysis results with $p < 0.05$ were considered
421 significant.
422
423 ***Analysis of published datasets***
424 Time series of single-cell data after bleomycin lung injury were obtained from the Tsukui and
425 Sheppard[42] and Strunz et al.[18] (GSE141259). These samples were processed and merged with Seurat
426 (4.3.0) using the function SCTransform to correct for batch effects and annotated with SingleR 1.10.044
427 using the ImmGen database as reference. We subsetted the macrophages from GSE141259[18]
428 repository and annotated by applying SingleR using as reference the macrophage subtypes (C1, C2,
429 C3) defined by Aran et al.[4] (GSE111664). Microarray RNA data from bronchoalveolar cells of healthy
430 individuals and IPF patients was extracted from the GPL14550 dataset within the GSE70867[21]
431 repository. The differentially expressed genes between IPF and healthy samples were obtained by

following the R workflow provided by the NCBI GEO2R platform using GEOquery(2.66.0) and limma (3.54.2) packages.

LC-MS metabolomics and ^{13}C-flux

Primary murine lung macrophages and fibroblasts were cocultured, or fibroblasts were cultures alone, as above, for 24 hours with or without 1mM $^{13}C_5$-ornithine (Cambridge Isotope Laboratories, CLM-4724-H-PK) or 1 mM CB-1158. Cell extracts were used to calculate protein equivalents by resuspension in 0.2 M NaOH, heated to 95 °C for 25 min, and determined via BCA (Pierce, 23225). Dried metabolites were resuspended in 50% ACN:water and 1/10th of the volume was loaded onto a Luna 3 um NH2 100A (150 × 2.0 mm) column (Phenomenex). The chromatographic separation was performed on a Vanquish Flex (Thermo Scientific) with mobile phases A (5 mM NH_4AcO pH 9.9) and B (ACN) and a flow rate of 200 µL/min. A linear gradient from 15% A to 95% A over 18 min was followed by 9 min isocratic flow at 95% A and reequilibration to 15% A. Metabolites were detected with a Thermo Scientific Q Exactive mass spectrometer run with polarity switching (+3.5 kV / -3.5 kV) in full scan mode with an m/z range of 65-975. TraceFinder 4.1 (Thermo Scientific) was used to quantify the targeted metabolites by area under the curve using expected retention time and accurate mass measurements (< 5 ppm). Values were normalized to cell number and sample protein concentration. Relative amounts of metabolites were calculated by summing up the values for all isotopologues of a given metabolite. Fractional contribution (FC) of ^{13}C carbons to total carbon for each metabolite was calculated as previously described[43].

Data and code availability

Newly generated single-cell sequencing data will be made public on acceptance for publication.

458 **References**

459 1 Tsukui, T. *et al.* Collagen-producing lung cell atlas identifies multiple subsets with
460 distinct localization and relevance to fibrosis. *Nat Commun* **11**, 1920 (2020).
461 https://doi.org:10.1038/s41467-020-15647-5
462 2 Tsukui, T. a. S., D. Tracing the origin of pathologic pulmonary fibroblasts. *Biorxiv*
463 (2022). https://doi.org:https://doi.org/10.1101/2022.11.18.517147
464 3 Buechler, M. B. *et al.* Cross-tissue organization of the fibroblast lineage. *Nature* **593**,
465 575-579 (2021). https://doi.org:10.1038/s41586-021-03549-5
466 4 Aran, D. *et al.* Reference-based analysis of lung single-cell sequencing reveals a
467 transitional profibrotic macrophage. *Nat Immunol* **20**, 163-172 (2019).
468 https://doi.org:10.1038/s41590-018-0276-y
469 5 Larson-Casey, J. L., Deshane, J. S., Ryan, A. J., Thannickal, V. J. & Carter, A. B.
470 Macrophage Akt1 Kinase-Mediated Mitophagy Modulates Apoptosis Resistance and
471 Pulmonary Fibrosis. *Immunity* **44**, 582-596 (2016).
472 https://doi.org:10.1016/j.immuni.2016.01.001
473 6 Satoh, T. *et al.* Identification of an atypical monocyte and committed progenitor involved
474 in fibrosis. *Nature* **541**, 96-101 (2017). https://doi.org:10.1038/nature20611
475 7 Meinken, J., Walker, G., Cooper, C. R. & Min, X. J. MetazSecKB: the human and animal
476 secretome and subcellular proteome knowledgebase. *Database (Oxford)* **2015** (2015).
477 https://doi.org:10.1093/database/bav077
478 8 Roofeh, D. *et al.* Tocilizumab Prevents Progression of Early Systemic Sclerosis-
479 Associated Interstitial Lung Disease. *Arthritis Rheumatol* **73**, 1301-1310 (2021).
480 https://doi.org:10.1002/art.41668
481 9 Group, R. C. Tocilizumab in patients admitted to hospital with COVID-19 (RECOVERY):
482 a randomised, controlled, open-label, platform trial. *Lancet* **397**, 1637-1645 (2021).
483 https://doi.org:10.1016/S0140-6736(21)00676-0
484 10 Khanna, D. *et al.* Tocilizumab in systemic sclerosis: a randomised, double-blind,
485 placebo-controlled, phase 3 trial. *Lancet Respir Med* **8**, 963-974 (2020).
486 https://doi.org:10.1016/S2213-2600(20)30318-0
487 11 Narvaez, J. *et al.* Effectiveness and safety of tocilizumab for the treatment of refractory
488 systemic sclerosis associated interstitial lung disease: a case series. *Ann Rheum Dis*
489 **78**, e123 (2019). https://doi.org:10.1136/annrheumdis-2018-214449
490 12 Riteau, N. *et al.* Extracellular ATP is a danger signal activating P2X7 receptor in lung
491 inflammation and fibrosis. *Am J Respir Crit Care Med* **182**, 774-783 (2010).
492 https://doi.org:10.1164/rccm.201003-0359OC
493 13 Bhattacharyya, A. *et al.* Macrophage Cx43 Is Necessary for Fibroblast Cytosolic
494 Calcium and Lung Fibrosis After Injury. *Front Immunol* **13**, 880887 (2022).
495 https://doi.org:10.3389/fimmu.2022.880887
496 14 Trang, T., Beggs, S., Wan, X. & Salter, M. W. P2X4-receptor-mediated synthesis and
497 release of brain-derived neurotrophic factor in microglia is dependent on calcium and
498 p38-mitogen-activated protein kinase activation. *J Neurosci* **29**, 3518-3528 (2009).
499 https://doi.org:10.1523/JNEUROSCI.5714-08.2009
500 15 Le Guilcher, C. *et al.* The P2X4 purinergic receptor regulates hepatic myofibroblast
501 activation during liver fibrogenesis. *J Hepatol* **69**, 644-653 (2018).
502 https://doi.org:10.1016/j.jhep.2018.05.020

16 Dichtl, S. *et al.* Lactate and IL6 define separable paths of inflammatory metabolic adaptation. *Sci Adv* **7** (2021). https://doi.org:10.1126/sciadv.abg3505
17 Jin, S. *et al.* Inference and analysis of cell-cell communication using CellChat. *Nat Commun* **12**, 1088 (2021). https://doi.org:10.1038/s41467-021-21246-9
18 Strunz, M. *et al.* Alveolar regeneration through a Krt8+ transitional stem cell state that persists in human lung fibrosis. *Nat Commun* **11**, 3559 (2020). https://doi.org:10.1038/s41467-020-17358-3
19 Fabre, T. *et al.* Identification of a broadly fibrogenic macrophage subset induced by type 3 inflammation. *Sci Immunol* **8**, eadd8945 (2023). https://doi.org:10.1126/sciimmunol.add8945
20 Steggerda, S. M. *et al.* Inhibition of arginase by CB-1158 blocks myeloid cell-mediated immune suppression in the tumor microenvironment. *J Immunother Cancer* **5**, 101 (2017). https://doi.org:10.1186/s40425-017-0308-4
21 Prasse, A. *et al.* BAL Cell Gene Expression Is Indicative of Outcome and Airway Basal Cell Involvement in Idiopathic Pulmonary Fibrosis. *Am J Respir Crit Care Med* **199**, 622-630 (2019). https://doi.org:10.1164/rccm.201712-2551OC
22 Tharp, K. M. *et al.* Myeloid mechano-metabolic programming restricts anti-tumor immunity. *bioRxiv*, 2022.2007.2014.499764 (2022). https://doi.org:10.1101/2022.07.14.499764
23 Tran, D. H. *et al.* Mitochondrial NADP(+) is essential for proline biosynthesis during cell growth. *Nat Metab* **3**, 571-585 (2021). https://doi.org:10.1038/s42255-021-00374-y
24 Bhattacharya, M. & Ramachandran, P. Immunology of human fibrosis. *Nat Immunol* (2023). https://doi.org:10.1038/s41590-023-01551-9
25 Zepp, J. A. *et al.* Distinct Mesenchymal Lineages and Niches Promote Epithelial Self-Renewal and Myofibrogenesis in the Lung. *Cell* **170**, 1134-1148 e1110 (2017). https://doi.org:10.1016/j.cell.2017.07.034
26 Stancil, I. T. *et al.* Interleukin-6-dependent epithelial fluidization initiates fibrotic lung remodeling. *Sci Transl Med* **14**, eabo5254 (2022). https://doi.org:10.1126/scitranslmed.abo5254
27 Mauer, J. *et al.* Signaling by IL-6 promotes alternative activation of macrophages to limit endotoxemia and obesity-associated resistance to insulin. *Nat Immunol* **15**, 423-430 (2014). https://doi.org:10.1038/ni.2865
28 Foo, S. S. *et al.* Ephrin-B2 controls cell motility and adhesion during blood-vessel-wall assembly. *Cell* **124**, 161-173 (2006). https://doi.org:10.1016/j.cell.2005.10.034
29 Clausen, B. E., Burkhardt, C., Reith, W., Renkawitz, R. & Forster, I. Conditional gene targeting in macrophages and granulocytes using LysMcre mice. *Transgenic Res* **8**, 265-277 (1999). https://doi.org:10.1023/a:1008942828960
30 Ozaki, T. *et al.* The P2X4 receptor is required for neuroprotection via ischemic preconditioning. *Sci Rep* **6**, 25893 (2016). https://doi.org:10.1038/srep25893
31 El Kasmi, K. C. *et al.* Toll-like receptor-induced arginase 1 in macrophages thwarts effective immunity against intracellular pathogens. *Nat Immunol* **9**, 1399-1406 (2008). https://doi.org:10.1038/ni.1671
32 Reese, T. A. *et al.* Chitin induces accumulation in tissue of innate immune cells associated with allergy. *Nature* **447**, 92-96 (2007). https://doi.org:10.1038/nature05746
33 Kopf, M. *et al.* Impaired immune and acute-phase responses in interleukin-6-deficient mice. *Nature* **368**, 339-342 (1994). https://doi.org:10.1038/368339a0

549 34 Yata, Y. *et al.* DNase I-hypersensitive sites enhance alpha1(I) collagen gene expression
550 in hepatic stellate cells. *Hepatology* **37**, 267-276 (2003).
551 https://doi.org:10.1053/jhep.2003.50067
552 35 Bankhead, P. *et al.* QuPath: Open source software for digital pathology image analysis.
553 *Sci Rep* **7**, 16878 (2017). https://doi.org:10.1038/s41598-017-17204-5
554 36 Hao, Y. *et al.* Integrated analysis of multimodal single-cell data. *Cell* **184**, 3573-3587
555 e3529 (2021). https://doi.org:10.1016/j.cell.2021.04.048
556 37 McGinnis, C. S., Murrow, L. M. & Gartner, Z. J. DoubletFinder: Doublet Detection in
557 Single-Cell RNA Sequencing Data Using Artificial Nearest Neighbors. *Cell Syst* **8**, 329-
558 337 e324 (2019). https://doi.org:10.1016/j.cels.2019.03.003
559 38 Heng, T. S., Painter, M. W. & Immunological Genome Project, C. The Immunological
560 Genome Project: networks of gene expression in immune cells. *Nat Immunol* **9**, 1091-
561 1094 (2008). https://doi.org:10.1038/ni1008-1091
562 39 Chen, E. Y. *et al.* Enrichr: interactive and collaborative HTML5 gene list enrichment
563 analysis tool. *BMC Bioinformatics* **14**, 128 (2013). https://doi.org:10.1186/1471-2105-14-
564 128
565 40 Gene Ontology, C. *et al.* The Gene Ontology knowledgebase in 2023. *Genetics* **224**
566 (2023). https://doi.org:10.1093/genetics/iyad031
567 41 Kramer, A., Green, J., Pollard, J., Jr. & Tugendreich, S. Causal analysis approaches in
568 Ingenuity Pathway Analysis. *Bioinformatics* **30**, 523-530 (2014).
569 https://doi.org:10.1093/bioinformatics/btt703
570 42 Tsukui, T. & Sheppard, D. Tracing the origin of pathologic pulmonary fibroblasts.
571 *bioRxiv*, 2022.2011.2018.517147 (2022). https://doi.org:10.1101/2022.11.18.517147
572 43 Robinson, M. D. & Oshlack, A. A scaling normalization method for differential
573 expression analysis of RNA-seq data. *Genome Biol* **11**, R25 (2010).
574 https://doi.org:10.1186/gb-2010-11-3-r25
575 44 Satija, R., Farrell, J. A., Gennert, D., Schier, A. F. & Regev, A. Spatial reconstruction of
576 single-cell gene expression data. *Nat Biotechnol* **33**, 495-502 (2015).
577 https://doi.org:10.1038/nbt.3192
578 45 Taylor S. Adams, J. C. S., Sergio Poli, Ehab A. Ayaub, Nir Neumark, Farida
579 Ahangari, Sarah G. Chu, Benjamin A. Raby, Giuseppe DeIuliis, Michael Januszyk,
580 Qiaonan Duan, Heather A. Arnett, Asim Siddiqui, George R. Washko, Robert Homer,
581 Xiting Yan, Ivan O. Rosas, Naftali Kaminski. Single Cell RNA-seq reveals ectopic and
582 aberrant lung resident cell populations in Idiopathic Pulmonary Fibrosis. *Biorxiv* **doi:**
583 **https://doi.org/10.1101/759902** (2019).
584

585 **Acknowledgements**

586 This work was supported by funding from the US Department of Defense (Grant W81XWH2110417 to
587 MB), the UCSF Bakar Aging Research Institute (Investigator Grant to MB), and Longevity Impetus
588 Grants from Norn Group (MB and JGO). The authors would like to acknowledge the staff within the
589 Biological Imaging Development CoLab (BIDC) at UCSF Parnassus Heights, particularly Kyle Marchuk

590 and Austin Edwards, for their support in microscopy experiments. Sequencing performed at the UCSF
591 CAT was supported by UCSF PBBR, RRP IMIA, and NIH 1S10OD028511-01.
592

593 **Author contributions**

594 PY and JGO performed or assisted in the analysis of all the experiments and in figure preparation. KC
595 and CP performed single cell library preparation and sequencing, supervised by ARA. NB and AB
596 assisted in functional experiments with lung tissues and cells. XY performed human cell coculture
597 experiments. JN performed flow cytometry of mouse lung cells supervised by ABM. KB performed
598 mouse breeding and development of crosses for experiments. TT and DS performed single cell
599 sequencing of mouse lung fibroblasts. MM and HT provided deceased donor control lung tissues
600 supervised by MAM. RM generated and provided P2x4 floxed mice. MN performed
601 immunofluorescence analysis of IPF lung tissues. PJW provided lung explants from IPF patients and
602 helped to interpret associated imaging data. KMT designed and performed metabolomic assays,
603 assisted by PY. MB conceived of the work, supervised experimental planning and execution, and wrote
604 the manuscript with input from PJW, KT, MM, DS, and TT.
605

606 **Competing Interests**

607 The authors declare that there are no competing interests.
608

609 **Materials and Correspondence**

610 Correspondence to mallar.bhattacharya@ucsf.edu.
611
612

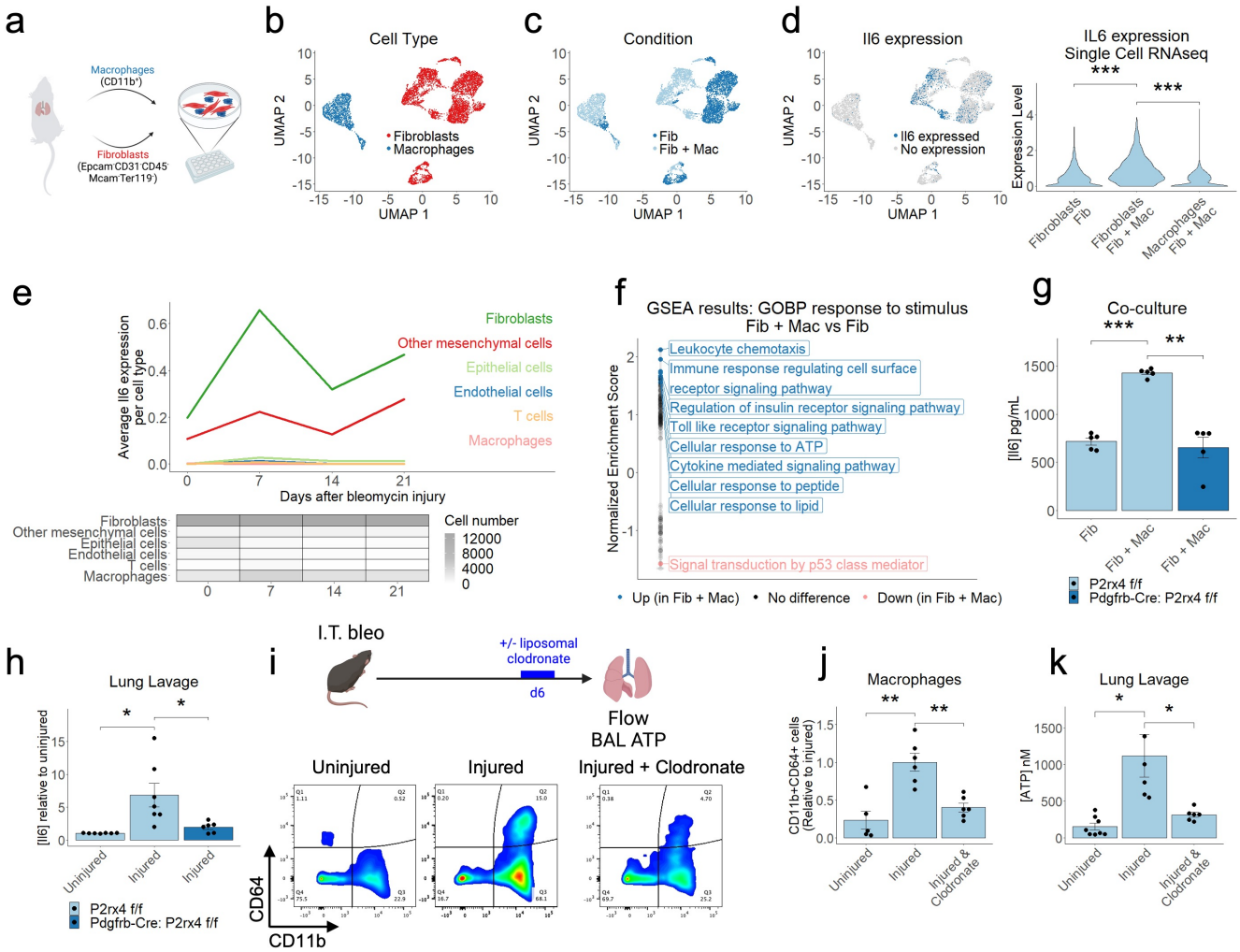

Figure 1: Extracellular ATP signaling induces fibroblast IL-6 expression.

(a) Schematic of scRNAseq of primary lung macrophage and fibroblast coculture.

(b) UMAP plot of scRNAseq for macrophage-fibroblast cocultures with SingleR-based cell type annotation[4] shown. Data represent n=2 separate cultures for each condition.

(c) UMAP plot for data from (b) showing sample of origin (left; "Fib"=fibroblast monoculture, "Fib + Mac"= fibroblast coculture with macrophages).

(d) Left: UMAP plot showing *Il6* expression. Right: Violin plot of *Il6 expression*. ***p<0.001 by Wilcoxon Rank Sum test corrected for multiple comparisons by Bonferroni method.

(e) Quantification of *Il6* expression by cell type in cells sequenced by scRNAseq directly after isolation from the lung at steady state and multiple time points after injury (reanalysis of merged data[18,42] normalized by Sctransform[44]).

(f) Gene set enrichment analysis (GSEA) of fibroblast single cell transcriptomes in coculture with macrophages compared to fibroblast monoculture using GO "Response to stimulus" pathways.

(g) IL-6 ELISA of conditioned media from macrophage-fibroblast cocultures with or without fibroblast-specific P2rx4 deletion. N=5 five biological replicates per condition. **p<0.01, ***p<0.001 by Student's t-test.

(h) IL-6 ELISA from bronchoalveolar lavage form mice with or without fibroblast-specific P2rx4 deletion. N=7, 7, 6 biological replicates, left to right. *p<0.05 by Student's t-test.

633 (i) Schematic for macrophage depletion and representative flow cytometry for CD11b+CD64+
634 macrophages with and without bleomycin injury and intratracheal clodronate treatment.
635 (j) CD11b+CD64+ macrophages with and without injury and liposomal clodronate treatment. N=5,
636 6, 6 biological replicates, left to right. **$p<0.01$ by Student's t-test.
637 (k) Bronchoalveolar lavage ATP concentrations. N=8, 5, 6 biological replicates, left to right. *$p<0.05$
638 by Student's t-test.
639
640

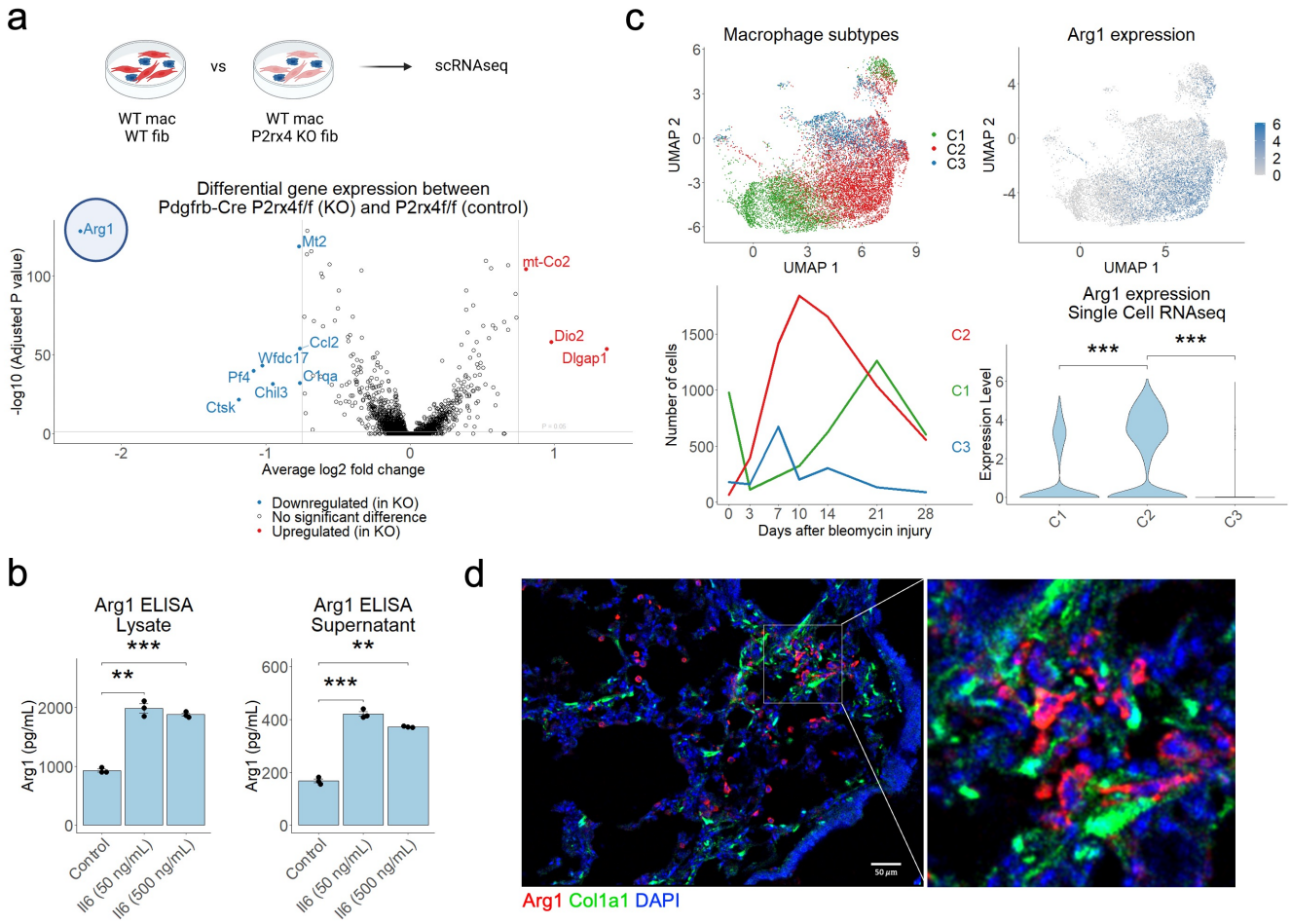

Figure 2: Transitional macrophages express Arg1, an IL-6 inducible gene.

(a) Top: Schematic of design of co-culture scRNAseq. Bottom: Volcano plot for macrophages from scRNAseq of macrophage-fibroblast cocultures for WT macrophages and fibroblasts, or WT macrophages cocultured with P2rx4 KO (*Pdgfrb-Cre: P2rx4 f/f*) fibroblasts. Significance was determined by Wilcoxon Rank Sum test corrected for multiple comparisons by Bonferroni method. Color-labeled genes had $p<0.05$ and absolute value of log log2 fold change >0.75. Data represent n=2 separate cocultures.

(b) Arg1 ELISA of cell lysates and conditioned media collected from mouse lung macrophage monoculture 72 hours after IL-6 treatment. N=3 biological replicates per condition.**$p<0.01$, ***$p<0.001$ by Student's t-test.

(c) Analysis of macrophages from bleomycin lung injury (data reanalyzed from Strunz et al.[18]). Top left: Annotation of macrophages from multiple time points, according to C1, C2, or C3 macrophage annotation (as described in Aran et al.[4]; C1=alveolar macrophages; C2=transitional monocyte-derived macrophages; C3=monocyte derived macrophages). Top right: Feature plot of Arg1 expression. Bottom left: Proportions of C1, C2, and C3 across time. Bottom right: Violin plot of Arg1 expression according to cluster (C1, C2, and C3).

(d) Immunofluorescence of *Col1a1-GFP* mice labeled with Arg1 antibody at 14 days after bleomycin injury.

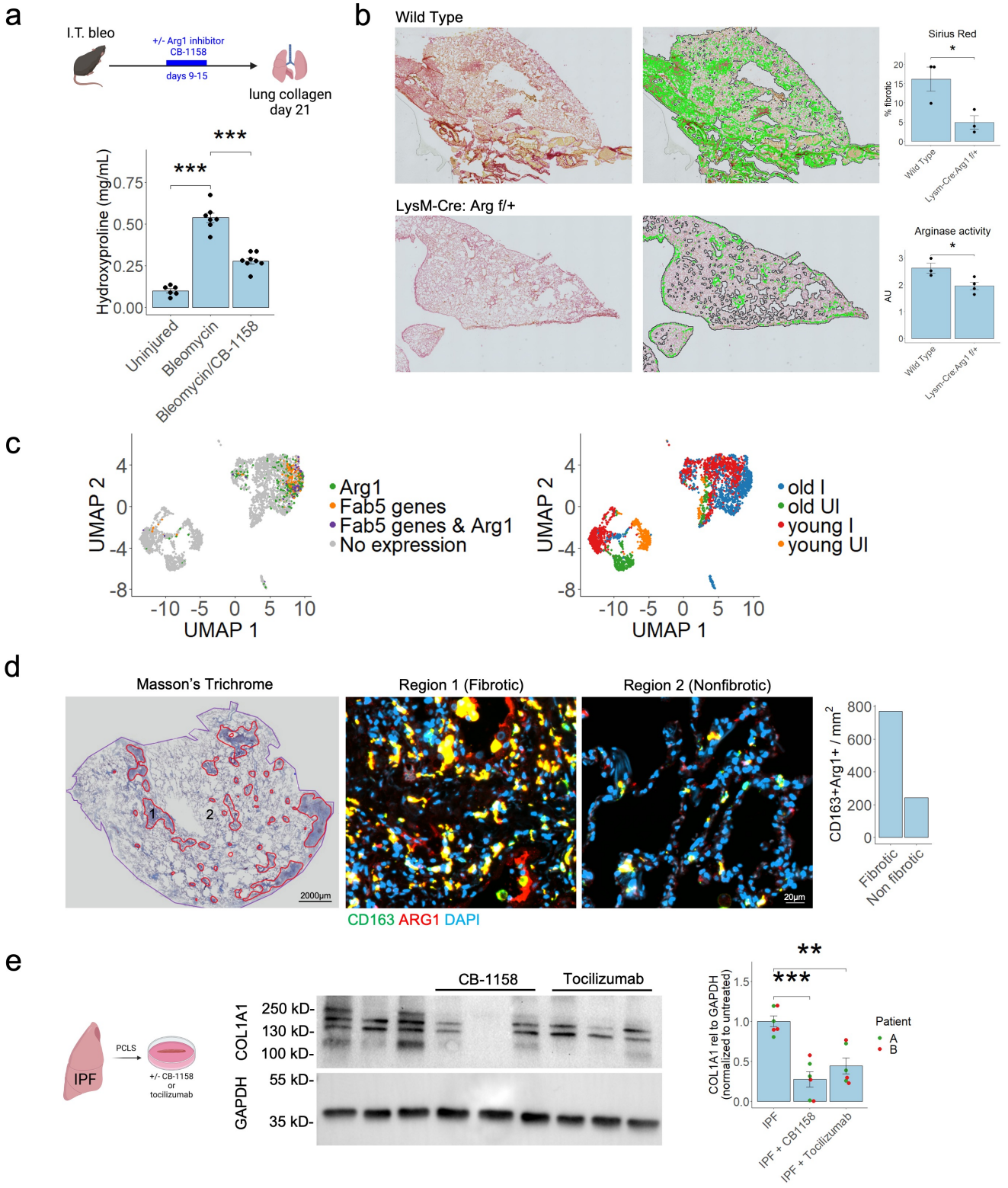

Figure 3: Arg1 is necessary for fibrosis in murine and human lung.

666 (a) Hydroxyproline assay for collagen content of lungs from injured and uninjured WT mice treated
667 with or without Arg1 inhibitor CB-1158 during days 9-15 post bleomycin. N=6, 7, 8 mice, left to
668 right. ***p<0.001 by Student's t-test.
669 (b) Representative images of Sirius red stain for collagen in injured WT or Lysm-Cre:Arg1 f/+ mice
670 at 14 days post-bleomycin, with fibrotic regions highlighted in green for the same images.
671 Results for n=3 mice per condition are quantified in the plot. Lung lysate arginase activity was
672 quantified at 14 days post injury (n=3 and 4 mice per condition, left to right). *p<0.05 by
673 Student's t-test.
674 (c) UMAP of macrophages identified by SingleR[4] from CD45+ cells directly isolated by antibody
675 column and sequenced by scRNAseq after bleomycin injury from aged (96-week-old) and young
676 (6-8 week old) mice. Cells expressing Arg1 were defined as cells having >1 counts after scaling
677 and centering[44]. Cells expressing Fab5 genes were defined as cells whose average expression
678 of *Trem2*, *Cd9*, *Spp1*, *Gpnmb*, and *Fabp5*[19] was >1 after scaling and centering. N=2 mice per
679 condition. UI=uninjured. I=injured.
680 (d) Masson's trichrome and immunofluorescence images from sections of IPF lung (images shown
681 are representative of 4 separate IPF patient lung samples). Immunofluorescence images were
682 taken from an adjacent section and correspond to the fibrotic (Region 1) and nonfibrotic (Region
683 2) areas indicated in the Masson's trichrome image. Cellular content was quantified in fibrotic
684 regions (indicated in red) versus the remaining nonfibrotic area.
685 (e) Immunoblot for COL1A1 from lung slice lysates prepared 24 hours after treatment in culture with
686 the indicated inhibitors. **p<0.01, ***p<0.001 by Student's t-test.
687

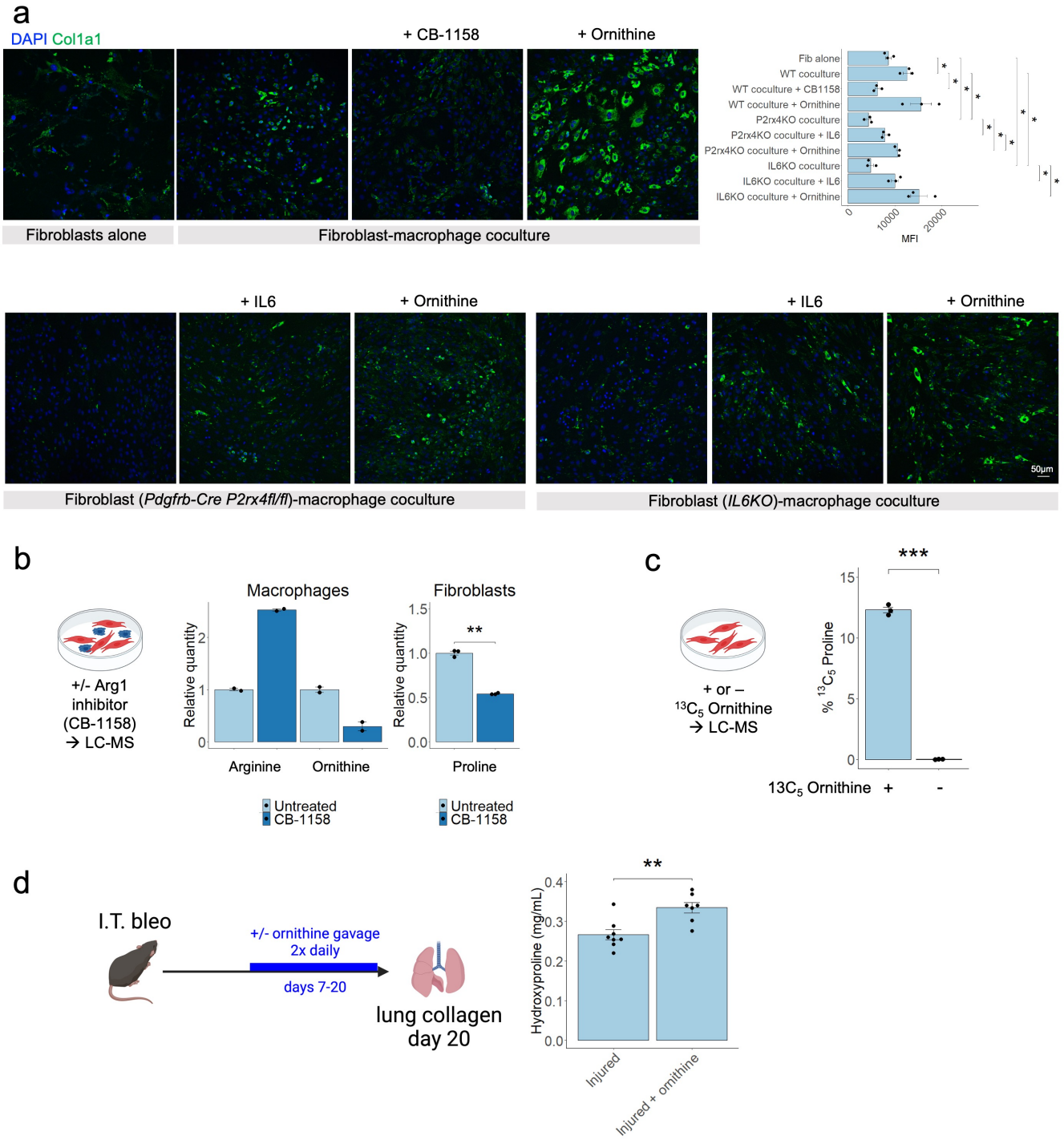

Figure 4: Macrophage Arg1 regulates fibroblast collagen expression via ornithine loading.

(a) Col1a1 immunofluorescence of mouse fibroblast cocultures or macrophage-fibroblast cocultures with or without CB-1158, IL-6, or ornithine treatment. N=3 biological replicates per condition. *p<0.05 by Student's t-test corrected for multiple comparisons by Bonferroni method.

(b) Relative quantities arginine, ornithine, proline in lysates of murine primary lung fibroblasts or macrophages, isolated after coculture with or without CB-1158 inhibitor treatment, quantified by

695 liquid chromatography-mass spectrometry. N=2 and 3 biological replicates for macrophages
696 and fibroblasts, respectively. **p<0.01 by Student's t-test.
697 (c) $^{13}C_5$ proline as a fraction of total proline quantified by liquid chromatography-mass spectrometry
698 from fibroblast lysates prepared after fibroblast monoculture, with or without treatment with $^{13}C_5$
699 ornithine for 24 hours. N=3 biological replicates per condition. ***p<0.001 by Student's t-test.
700 (d) Hydroxyproline assay for collagen content of lungs from injured WT mice treated with or without
701 ornithine (2 mg/kg) twice daily by ornithine gavage during days 7 through 20 . N=8, 7 mice, left
702 to right. **p<0.01 by Student's t-test.
703
704

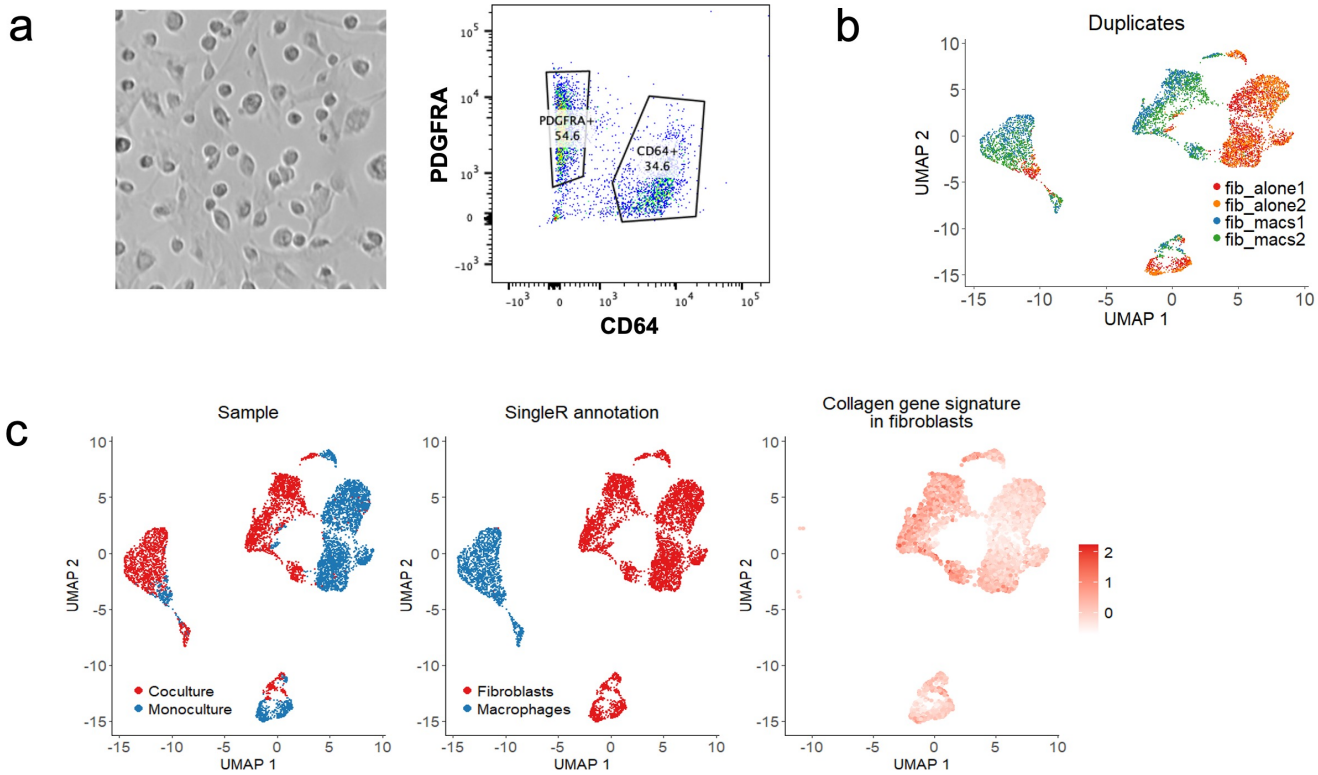

Supplementary Figure 1

(a) Left: Bright field image of cocultured primary macrophages and fibroblasts. Right: Flow cytometry for Pdgfra and CD64 with coculture cells.

(b) UMAP plot of replicates from culture-cell scRNAseq (n=2 separate cultures per condition).

(c) UMAPs of cultured-cell scRNAseq shown in Figure 1a-b labeled by culture condition, cell type annotated by SingleR, and collagen gene signature score (see Table 1 for genes).

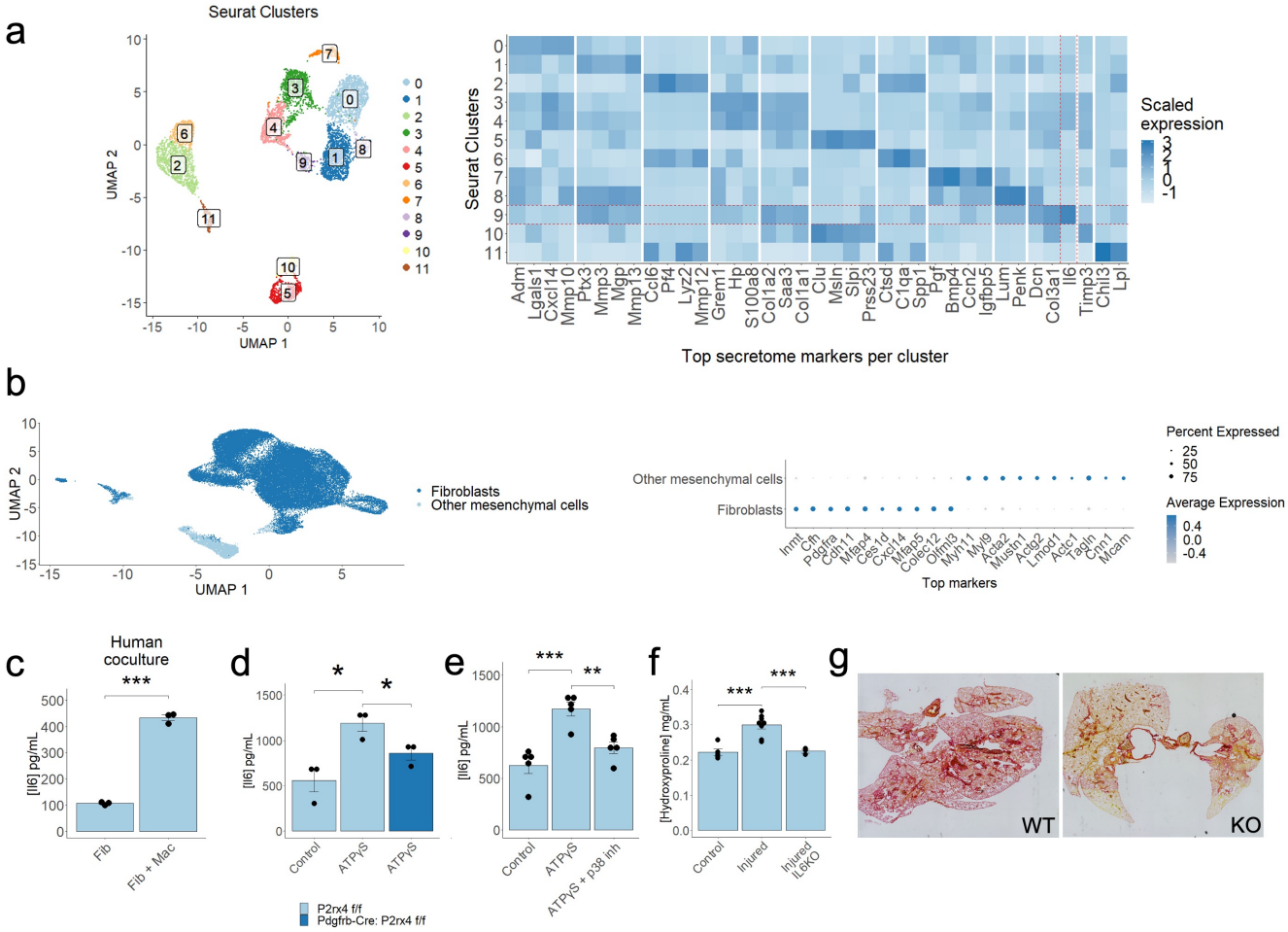

Supplementary Figure 2

(a) Heat map of the most highly expressed genes that are predicted to be secreted factors[7] by Seurat clustering shown. Clusters 3,4, 9, fibroblast clusters present only with macrophage coculture, expressed the highest *Il6*.

(b) UMAP of "Fibroblasts" and "Other mesenchymal cells" from Figure 1e (reanalysis of scRNAseq data[18,42]), and dot plot of top differentially expressed genes showing that Other mesenchymal cells express multiple smooth muscle (eg *Myh11*, *Myl9*, *Acta2*, and *Tagln*) and pericyte markers (eg, *Mcam*).

(c) IL-6 ELISA from conditioned media from deceased donor human lung macrophage-fibroblast coculture. N=3 biological replicates per condition. ***p<0.001 by Student's t-test.

(d) IL-6 ELISA of conditioned media from monocultured mouse lung fibroblasts from fibroblast-specific P2rx4 KO (Pdgfrb-Cre: P2rx4 f/f) or WT mice, with and without ATPγS treatment. N=3 biological replicates per condition. *p<0.05 by Student's t-test.

(e) IL-6 ELISA of conditioned media from monocultured mouse lung fibroblasts with and without ATPγS and SB203580 (p38 Map Kinase inhibitor) treatment. N=5 biological replicates per condition. **p<0.01, ***p<0.001 by Student's t-test.

(f) Hydroxyproline assay for WT and Il6 KO mice at 21 days after bleomycin injury. N=5, 8, and 3 mice, left to right. ***p<0.001 by Student's t-test.

(g) Sirius Red staining for WT and Il6 KO mice at 21 days after bleomycin injury (representative images; n=2 in each condition).

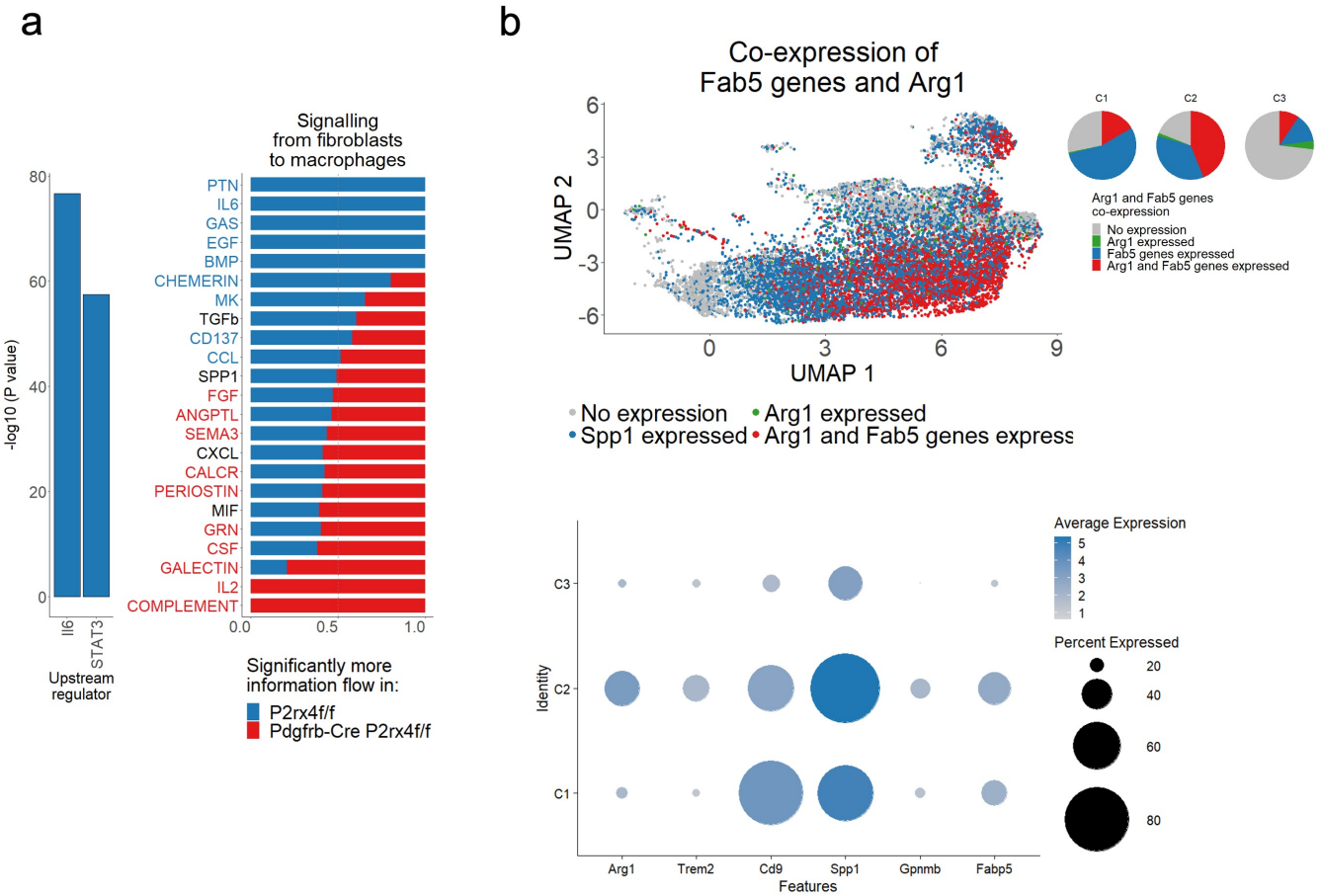

Supplementary Figure 3

(a) Left: Ingenuity Pathways Analysis of predicted upstream regulators for macrophages cultured with WT relative to P2rx4 fibroblasts. Right: CellChat plot comparing WT and P2rx4 conditions for data from Figure 2a. Significance was determined by Wilcoxon test with $p<0.05$.

(b) Top: Feature plot of macrophages from Strunz et al.[18] with Arg1 and Spp1 expression as well as Fab5 profibrotic macrophage genes[19] indicated. Bottom: proportions of expression by C1, C2, or C3 annotation. Bottom: Dot plot for gene expression of cells from Strunz et al.[18] annotated as either C1, C2, or C3 macrophages (left; C1=alveolar macrophages; C2=transitional monocyte-derived macrophages; C3=monocyte derived macrophages, nomenclature per Aran et al.[4]).

a

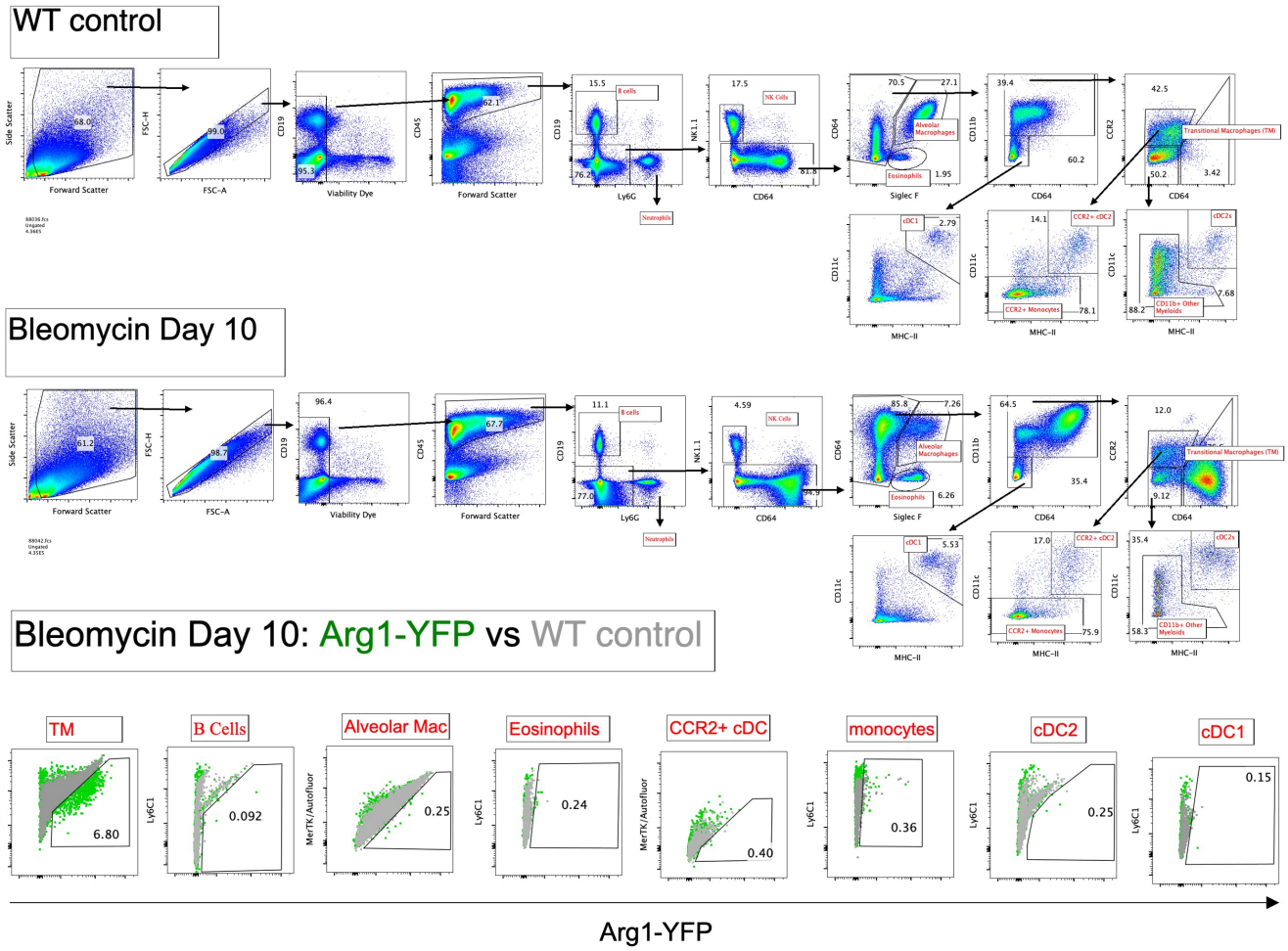

b

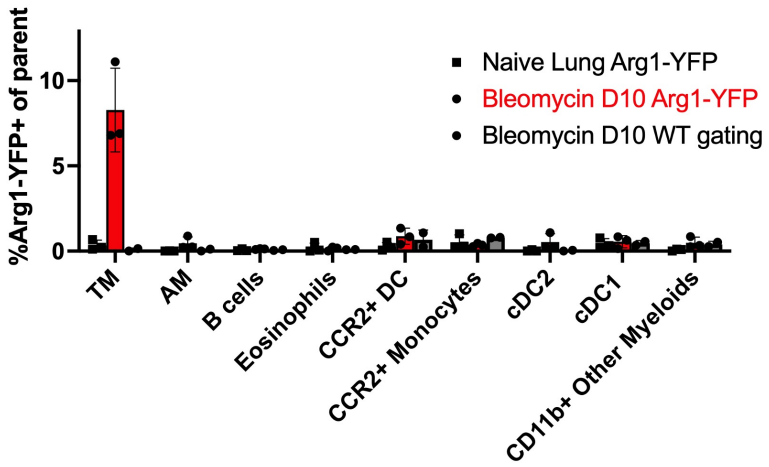

Supplementary Figure 4

753 (a) Gating strategy for mice at steady state and 10 days post-bleomycin. TM=transitional
754 macrophage (CD64+CD11b+ SiglecF-, as shown). AM=alveolar macrophage (CD64+SiglecF+,
755 as shown).
756 (b) Plot of percentage of cells expressing YFP in each lineage. N=3 mice per condition.
757
758

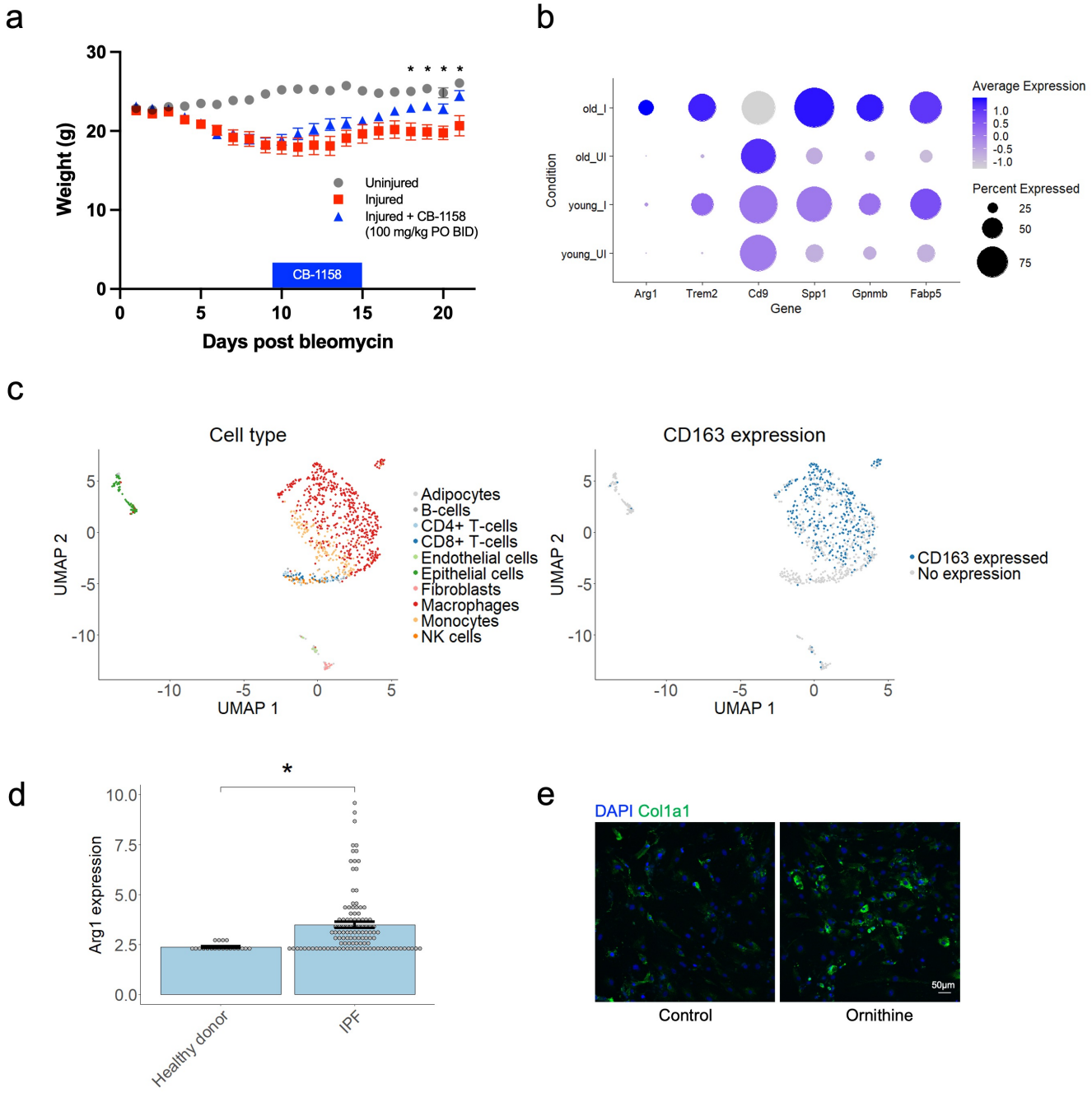

Supplementary Figure 5

(a) Weight measured daily in CB-1158-treated mice (corresponding to Figure 3a). *p<0.05 by Student's t-test.

(b) Dot plot of Fab5[19] gene expression in old and young mouse lung macrophages after bleomycin injury (corresponding to Figure 3c). UI=uninjured. I=injured.

(c) UMAPs of ARG1-expressing cells identified from human lung scRNAseq[45]. SingleR cell type annotations of these cells and a feature plot of the macrophage marker CD163 is shown.

(d) ARG1 expression by microarray analysis of gene expression of BAL cells from healthy (20 patients) and IPF (112 patients) from GSE70867[21].

770 (e) Col1a1 immunofluorescence of monocultured lung fibroblasts with or without ornithine
771 treatment.
772

773

Table S1: Collagen genes used for collagen gene score (corresponding to Figure S1b)

Col1a1
Col1a2
Col3a1
Col4a1
Col4a2
Col4a4
Col5a1
Col5a3
Col6a3
Col6a6
Col8a1
Col9a3
Col10a1
Col13a1
Col15a1
Col22a1
Col23a1